



# HHS Public Access

Author manuscript

*Nat Med.* Author manuscript; available in PMC 2013 December 01.

Published in final edited form as:

*Nat Med.* 2013 June ; 19(6): 722–729. doi:10.1038/nm.3190.

## Hepatitis C Virus Infection Activates a Novel Innate Pathway Involving IKK $\alpha$ in Lipogenesis and Viral Assembly

Qisheng Li, Véronique Pène, Siddharth Krishnamurthy, Helen Cha, and T. Jake Liang

Liver Diseases Branch, National Institute of Diabetes and Digestive and Kidney Diseases, National Institutes of Health, Bethesda, MD 20892, USA

### Abstract

Hepatitis C virus interacts extensively with host factors not only to establish productive infection but also to trigger unique pathological processes. Our recent genome-wide siRNA screen demonstrated that IKK $\alpha$  is a critical host factor for HCV. Here we describe a novel NF- $\kappa$ B-independent and kinase-mediated nuclear function of IKK $\alpha$  in HCV assembly. HCV infection, through its 3'-untranslated region, interacts with DDX3X to activate IKK $\alpha$ , which translocates to the nucleus and induces a CBP/p300-mediated transcriptional program involving SREBPs. This novel innate pathway induces lipogenic genes and enhances core-associated lipid droplet formation to facilitate viral assembly. Chemical inhibitors of IKK $\alpha$  suppress HCV infection and IKK $\alpha$ -induced lipogenesis, offering a proof-of-concept approach for novel HCV therapeutic development. Our results show that HCV commands a novel mechanism to its advantage by exploiting intrinsic innate response and hijacking lipid metabolism, which likely contributes to a high chronicity rate and the pathological hallmark of steatosis in HCV infection.

---

Hepatitis C virus (HCV) infection is a leading cause of chronic liver disease associated with significant morbidity and mortality in the world<sup>1</sup>. To date a protective vaccine is not available, and current therapeutic regimen is suboptimal<sup>2</sup>. The virus has a unique propensity to cause persistent infection and induce progressive liver damage<sup>3</sup>. HCV exploits extensively host factors such as cellular lipid metabolic pathways for efficient propagation<sup>4,5</sup>. HCV has been shown to alter lipid metabolism of infected hepatocytes<sup>6</sup>, conferring a unique pathological feature of HCV infection – hepatic steatosis. Activation of sterol regulatory element-binding proteins (SREBPs), critical transcriptional regulators of cholesterol and fatty acid metabolism<sup>7</sup>, has been shown in HCV-infected hepatocytes<sup>8,9</sup>. The mechanistic basis of these functional effects remains unclear.

HCV activates host innate immunity that functions to limit viral infection. Recognition of viral pathogen-associated molecular patterns (PAMPs) by pattern recognition receptor

---

Users may view, print, copy, download and text and data- mine the content in such documents, for the purposes of academic research, subject always to the full Conditions of use: [http://www.nature.com/authors/editorial\\_policies/license.html#terms](http://www.nature.com/authors/editorial_policies/license.html#terms)

Correspondence should be addressed to T.J.L. (jakel@bdg10.niddk.nih.gov).

#### AUTHOR CONTRIBUTIONS

Q.L. and T.J.L. conceived and designed the study. Q.L., V.P., S.K. and H.C. conducted experiments. Q.L., V.P. and T.J.L. analyzed data. Q.L. and T.J.L. wrote the paper with the input from V.P. T.J.L. supervised the studies.

#### COMPETING FINANCIAL INTERESTS

The authors declare no competing financial interests.

(PRR) like RIG-I-like receptors (RLRs) and activation of various signaling pathways including IRF3 and NF- $\kappa$ B represent early steps of intrinsic innate immune response, with subsequent induction of interferons<sup>10</sup>. The NF- $\kappa$ B pathway is tightly regulated by the I $\kappa$ B kinase (IKK) complex, which consists of two catalytic subunits, IKK $\alpha$  and IKK $\beta$ , and a regulatory subunit NEMO (IKK $\gamma$ )<sup>11</sup>. Activation of IKK $\beta$  and NEMO and subsequent I $\kappa$ B degradation are critical steps in the activation of the canonical NF- $\kappa$ B pathway<sup>12</sup>. IKK $\alpha$  preferentially phosphorylates NF- $\kappa$ B2 rather than I $\kappa$ B and leads to the activation of p52-RelB heterodimers that regulate a distinct subset of NF- $\kappa$ B target genes<sup>12</sup>. This alternative action is referred to as the non-canonical pathway<sup>13</sup>. IKK $\alpha$  is a remarkably versatile molecule involved in diverse and multiple signaling pathways to regulate gene expression; many of its actions are independent of NF- $\kappa$ B<sup>12,14</sup>. Unlike IKK $\beta$ , IKK $\alpha$  can shuttle between the cytoplasm and nucleus<sup>15,16</sup>. In the nucleus, IKK $\alpha$  interacts with CREB binding protein (CBP) and contributes to NF- $\kappa$ B-mediated gene expression through phosphorylation of histone H3<sup>15,17,18</sup>. The transcription targets of IKK $\alpha$ , however, remain largely unknown.

We recently performed a genome-wide RNA interference (RNAi) screen to discover HCV host dependencies. One of the highly host-dependent factors identified is IKK $\alpha$  (under the name CHUK)<sup>19</sup>. Here we show that IKK $\alpha$  is requisite for productive HCV infection and upregulates lipogenesis of host cells for efficient viral assembly via transcriptional induction of SREBPs. HCV infection, through the action of 3'-untranslated region (3'UTR), interacts with DDX3X to activate IKK $\alpha$  and hence induces LD biogenesis. Our study provides a direct functional link between HCV infection, inflammation, innate immunity and hepatic lipid metabolism.

## RESULTS

### Identification of IKK $\alpha$ as a Novel Host Factor Required for HCV Infection

We applied a two-part viral infection protocol to characterize host dependencies associated with both early (part-one) and late (part-two) stages of HCV life cycle<sup>19</sup>. The effect of IKK $\alpha$  silencing was more pronounced in part-two (>85% inhibition) than part-one (~60% inhibition), implicating that IKK $\alpha$  acts more on the late stage of viral infection (Fig. 1a and Supplementary Fig. 1a). The effect of IKK $\alpha$  depletion was confirmed by testing four individual siRNAs of the pool (Fig. 1b and Supplementary Fig. 1b). Expression of a siRNA-resistant IKK $\alpha$  mutant (HA-IKK $\alpha$  MUT) restored HCV infection in IKK $\alpha$  siRNA-treated cells (Supplementary Fig. 1c), further validating the phenotype-specific role of IKK $\alpha$  in HCV infection.

IKK $\alpha$  siRNA significantly impaired production and secretion of infectious HCV by more than ten folds (Fig. 1c). Over-expression of IKK $\alpha$  by transfecting HA-IKK $\alpha$  plasmid substantially increased infectious HCV production (Fig. 1d). IKK $\alpha$ 's function requires its kinase activity and IKK $\alpha$  kinase-defective mutant (IKK $\alpha$  KM) behaves like a dominant negative mutant<sup>20</sup>. Transfection of IKK $\alpha$  KM blocked HCV propagation similar to the effect of IKK $\alpha$  siRNA (Fig. 1e).

To further investigate the role of IKK $\alpha$  in HCV infection, various IKK inhibitors were tested in HCV-infected Huh7.5.1 cells and primary human hepatocytes (PHHs) (Fig. 1f-i and

Supplementary Fig. 2). Treatment of Huh7.5.1 cells with wedelolactone and IKK inhibitor XII, chemical inhibitors of both IKK $\alpha$  and  $\beta$ , drastically reduced HCV core protein staining and infectious viral particle production (Fig. 1f, g). Increasing concentrations of both compounds led to a dose-dependent decline in HCV RNA production and secretion in both Huh7.5.1 cells and PHHs that could not be accounted by cytotoxicity at high concentrations (Fig. 1h, i, and Supplementary Fig. 2b, c). BMS-345541, an IKK $\beta$ -specific inhibitor, had little effect on HCV production (Fig. 1f–i and Supplementary Fig. 2b, c).

### IKK $\alpha$ 's Role in HCV Assembly and Lipid Droplet Formation

To investigate the step of HCV life cycle where IKK $\alpha$  is required, we applied multiple virologic assays. IKK $\alpha$  silencing preferentially affected extracellular HCV RNA levels in HCVcc infection system (Fig. 1b). We therefore specifically examined single-cycle replication by transfecting genomic HCV RNA into CD81-deficient Huh7 cells (Huh7.25)<sup>21</sup> and showed that HCV replication was not affected by IKK $\alpha$  silencing (Fig. 2a). IKK $\alpha$  silencing had no effect on assays targeting individual steps of HCV life cycle including entry (HCV pseudovirus assay), translation (HCV IRES-driven reporter), and replication (subgenomic replicon) (Supplementary Fig. 3 and Fig. 2b), consistent with a predominant role of IKK $\alpha$  in the late stage of viral life cycle.

We thus hypothesized that IKK $\alpha$  is involved in the assembly or secretion of infectious viral particles. The lipid droplet has been shown to play a crucial role in HCV assembly<sup>22–24</sup>. As expected, HCV proteins, particularly core and NS5A, were observed in close proximity to LDs in HCV-infected cells (Fig. 2c and Supplementary Fig. 4a, b). Cells infected with HCV exhibited a marked increase of LD numbers, LD-positive area, LD fluorescence intensity and triglyceride contents, while IKK $\alpha$  silencing significantly blocked this increase (Fig. 2c and Supplementary Fig. 4b, c). In HCV-infected cells treated with IKK $\alpha$  siRNA, the core protein expression was modestly reduced, but more importantly, the association between core protein and the LD was diminished substantially (Fig. 2c and Supplementary Fig. 4b), suggesting that IKK $\alpha$  is important for the association of LD with HCV proteins during the assembly process. As expected, IKK inhibitors wedelolactone and XII but not BMS-345541, showed strong inhibition of LD formation and co-localization of core and LD (Supplementary Fig. 4d). IKK $\alpha$  over-expression also significantly increased the number, size and fluorescence intensity of LDs (Fig. 2d). Conversely, transfection of HA-IKK $\alpha$  KM mutant strongly reduced LD formation (Fig. 2d). Collectively, these data indicate that IKK $\alpha$  affects predominantly HCV-induced LD formation and viral assembly, although additional effect on secretion cannot be ruled out completely.

### HCV 3'UTR Mediates Activation of IKK $\alpha$ and LD Formation

To define the mechanism of HCV-responsive activation of IKK $\alpha$  and induction of lipogenesis, we examined the role of 3'UTR of viral genome, which contains a previously identified HCV PAMP molecule, a poly-U/C sequence<sup>25</sup>. Transfection of HCV 3'UTR RNA demonstrated a strong induction of LD formation, and IKK $\alpha$  silencing by siRNA markedly diminished HCV 3'UTR-mediated increase of LD content (Fig. 2e and Supplementary Fig. 5a). Poly(I:C), a synthetic PAMP, also enhanced LD formation (Supplementary Fig. 5a). Transfection of HA-IKK $\alpha$  plasmid and HCV 3'UTR RNA

together showed increased phosphorylated IKK $\alpha$ , whereas IKK $\alpha$  phosphorylation was not detected in cells transfected with HA-IKK $\alpha$  KM (Supplementary Fig. 5b). Therefore HCV infection induces LD biogenesis through viral RNA-triggered activation of an IKK $\alpha$ -dependent pathway.

### IKK $\alpha$ 's Function in HCV infection is Independent of NF- $\kappa$ B

IKK $\alpha$  is a component of IKK controlling NF- $\kappa$ B activation but it has also been implicated in NF- $\kappa$ B-independent functions<sup>12</sup>. To dissect the function of the NF- $\kappa$ B pathway in connection to IKK $\alpha$  in HCV infection, we first silenced four major factors of the NF- $\kappa$ B family (NF- $\kappa$ B1, NF- $\kappa$ B2, RELA, and RELB), and two essential IKK catalytic units for NF- $\kappa$ B activation (IKK $\beta$  and NEMO)<sup>11</sup> (Fig. 3a–c). We observed an increase of HCV infection and replication (Fig. 3a, b), which is opposite to the observed effect of IKK $\alpha$  silencing. Second, silencing of the above NF- $\kappa$ B genes did not affect IKK $\alpha$ -mediated induction of LD formation and enhancement of HCV propagation (Fig. 3d, e). Third, signals known to activate the NF- $\kappa$ B pathway, such as IL1- $\beta$  and lymphotoxin (LT) $\alpha/\beta$ , did not induce LD formation (Fig. 3f and Supplementary Fig. 5c). siRNA against LT $\beta$  (LTB) or its receptor (LTBR), known to be involved in non-canonical activation of NF- $\kappa$ B via IKK $\alpha$ <sup>12</sup>, had little or no effect on HCV replication or LD induction (Supplementary Fig. 5d–g).

### DDX3X's Role in HCV Assembly and LD Formation

We next explored the signaling pathway that mediates the specific effect of HCV 3'UTR on IKK $\alpha$  activation. RIG-I has been shown to be the key PRR for HCV PAMP that resides in the 3'UTR<sup>25</sup>. Because RIG-I is nonfunctional in Huh7.5.1 cells<sup>25</sup>, we tested the roles of two other RLRs – MDA5 and LGP2, the RLR signaling-adaptor molecule MAVS, and a major downstream cytosolic kinase TBK1. Depletion of these factors by siRNA had little or no effect on HCV infection- or HCV 3'UTR-triggered LD formation (Supplementary Fig. 6a–c). The effects on HCV infection were somewhat variable, with siMDA5 causing an increase and siLGP2 a modest decrease (Supplementary Fig. 6d), which we attribute to a positive role of MDA5 and a negative role of LGP2 in RLR signaling<sup>26</sup>.

We then investigated whether DDX1, a putative PRR sensing dsRNA<sup>27</sup>, is involved in HCV 3'UTR-mediated effects and showed that siDDX1 had no effect (Supplementary Fig. 6a–c). DDX3X, another DExD/H helicase, has recently been implicated in innate immunity<sup>28,29</sup>. DDX3X has been shown to be important for HCV infection<sup>30,31</sup>. It was also identified as a strong proviral factor in our genome-wide siRNA screen but affected more the late stage of viral life cycle<sup>19</sup>. Silencing of DDX3X led to a more profound inhibition in extracellular than intracellular HCV RNA level and a significant impairment of viral infectivity (Fig. 4a), whereas over-expression of DDX3X increased extracellular level of HCV RNA more than the intracellular level (Fig. 4b). Depletion of DDX3X also abrogated the induction of LD biogenesis mediated by HCV 3'UTR and core-LD association in the context of HCV infection (Supplementary Fig. 6a–c).

### DDX3X Interacts with HCV 3'UTR and Activates IKK $\alpha$ -mediated Lipogenesis

In HCV 3'UTR-treated or HCV-infected cells, DDX3X redistributed to form speckle-like cytoplasmic structures (Fig. 4c, d and Supplementary Fig. 7, 8a), albeit its overall expression

remained unaltered (Supplementary Fig. 8b, c). DDX3X co-localized specifically with transfected Cy3-labelled HCV 3'UTR RNA but not with the control RNA (Fig. 4c and Supplementary Fig. 7). HCV 3'UTR RNA but not the control RNA formed a complex with DDX3X in cell lysate (Fig. 4e). HCV 3'UTR or infection induced the formation of IKK $\alpha$  aggregates, which co-localized extensively with the DDX3X-HCV 3'UTR complexes (Fig. 4c, d and Supplementary Fig. 7a, 8d). Poly(I:C) also induces DDX3X-IKK $\alpha$  association (Supplementary Fig. 8d, e).

In HCV-infected cells, increased interaction of DDX3X and IKK $\alpha$  was verified by co-immunoprecipitation (Fig. 4f). Silencing of DDX3X markedly reduced the co-localization of HCV 3'UTR and IKK $\alpha$ , whereas siIKK $\alpha$  had no effect on the complex formation between HCV 3'UTR and DDX3X (Supplementary Fig. 7a), suggesting that interaction of HCV 3'UTR with DDX3X is required for the subsequent recruitment of IKK $\alpha$  to the complex. Silencing of MAVS, which has been suggested to interact with DDX3X in activation of innate immunity<sup>28,32</sup>, had no effect on the interaction of HCV 3'UTR, DDX3X and IKK $\alpha$  (Supplementary Fig. 7a). These data indicate that in HCV-infected Huh7.5.1 cells, DDX3X signals predominantly through the IKK $\alpha$ -mediated lipogenic pathway to play a proviral role in HCV propagation.

Previous studies showed that HCV core binds to and redistributes DDX3X to the viral assembly sites around LDs; however, this interaction appears to be dispensable for HCV replication<sup>33</sup>. In HCV-infected cells, redistributed DDX3X partially co-localized with core or LDs (Supplementary Fig. 8f). Treatment of Huh7.5.1 cells with HCV 3'UTR or poly(I:C) also induced DDX3X-IKK $\alpha$  association but the DDX3X-IKK $\alpha$  complexes did not localize to the LDs (Fig. 4g and Supplementary Fig. 8e). To confirm that core is not involved in this DDX3X-IKK $\alpha$  pathway, we studied a HCV mutant with a core amino acid substitution (F24Y) that abolishes its interaction with DDX3X<sup>33</sup>, and showed that in the absence of core-DDX3X binding, DDX3X-IKK $\alpha$  interaction is still induced by HCV infection without LD association (Fig. 4h and Supplementary Fig. 8g).

### HCV Induces IKK $\alpha$ Phosphorylation and Nuclear Translocation

We next examined the consequence of DDX3X-IKK $\alpha$  interaction induced by HCV infection. Huh7.5.1 cells were infected with HCV and harvested at varying times (4 to 72 h) for determination of IKK $\alpha$  gene expression. There was no change in either mRNA or protein levels of IKK $\alpha$  in the presence of HCV infection (Supplementary Fig. 9a, b). However, a significant increase in phosphorylated IKK $\alpha$  representing the active form of IKK $\alpha$  was noted 12–24 h after HCV infection (Fig. 5a and Supplementary Fig. 9c). IKK $\alpha$ , when activated, shuttles from the cytoplasm to nucleus<sup>15,16</sup>. We examined the distribution of IKK $\alpha$  in nuclear and cytosolic fractions of HCV-infected cells. HCV infection by 12 h resulted in a marked nuclear accumulation of IKK $\alpha$  (Fig. 5b). As expected, treatment of cells with TNF- $\alpha$ , a bona fide activator of IKK $\alpha$ <sup>15</sup>, significantly enhanced IKK $\alpha$ 's phosphorylation and nuclear translocation, while the overall expression of IKK $\alpha$  remained unchanged (Fig. 5a, b and Supplementary Fig. 9b). Confocal microscopy confirmed nuclear accumulation of IKK $\alpha$  in HCV-infected or HCV 3'UTR-transfected cells (Fig. 5c and Supplementary Fig. 9d, e), and these cells displayed speckle-like association of IKK $\alpha$  and

DDX3X (Fig. 5c), and elevated LD contents (Supplementary Fig. 9e, f), whereas the majority of IKK $\alpha$  resided in the cytoplasm of uninfected cells. Phosphorylation of IKK $\alpha$  is required for its nuclear translocation because HA-IKK $\alpha$  KM mutant did not show nuclear localization (Supplementary Fig. 9g).

### **IKK $\alpha$ Activation Induces SREBP-Mediated Lipogenesis and LD Formation**

We performed microarray gene expression profiling and identified cellular genes that are transcriptionally regulated by IKK $\alpha$ . Huh7.5.1 cells were treated with either non-targeting (NT) control or IKK $\alpha$  siRNA in the absence or presence of HCV infection (four conditions). The knockdown efficiency of IKK $\alpha$  and effect on HCV infection were confirmed by measuring IKK $\alpha$  mRNA and HCV RNA levels (Supplementary Fig. 10a, b). Lipogenic genes, particularly SREBPs and SREBP target genes involved in fatty acid and triglyceride synthesis were upregulated by HCV, and their inductions were abrogated in IKK $\alpha$ -silenced cells (Fig. 5d and Supplementary Fig. 10c–i). Over-expression of IKK $\alpha$  WT or KM mutant, upregulated and downregulated the expression of SREBPs, respectively (Supplementary Fig. 10j). Under our experimental conditions, the effects of HCV infection and transfection tend to be underestimated, because the efficiency of infection and transfection is only about 40–50% of cells under the best circumstance.

We compared our microarray data set with a recent publication, which identified all SREBP-1-regulated lipid metabolism and human hepatic genes<sup>34</sup>. We showed that the genes regulated by SREBP-1 are significantly affected by HCV infection or IKK $\alpha$  silencing (Supplementary Fig. 10k, l), implying that IKK $\alpha$  plays a major role in SREBP-1 regulation of hepatic lipid metabolism genes. We further demonstrated that SREBP knockdown has a similar effect as IKK $\alpha$  silencing on HCV infection. After depletion of SREBP-1 and -2, there was a significant impairment of HCV production (Fig. 5e), likely stemming from the apparent diminution of LD formation (Fig. 5f). IKK $\alpha$  silencing and IKK inhibitors (wedelolactone and XII) also abrogated HCV 3'UTR-induced SREBP induction (Fig. 5g and Supplementary Fig. 10i). In PHHs, IKK inhibitors significantly reduced the mRNA levels of SREBP-1 and -2 (Supplementary Fig. 10m). As expected, silencing of DDX3X, IKK $\alpha$ , SREBP-1 or -2 in PHHs led to a significant reduction of extracellular than intracellular HCV RNA levels (Supplementary Fig. 11a, b).

### **IKK $\alpha$ Induces Expression of SREBP through CBP/p300**

Activated IKK $\alpha$  has been shown to phosphorylate CBP and upregulates its activities in the nucleus<sup>18</sup>. CBP/p300 is also involved in SREBP transcriptional activity<sup>35,36</sup>. CBP/p300 over-expression dramatically upregulates the expression of both SREBP-1 and SREBP-2<sup>37</sup>. We showed that both IKK $\alpha$  and CBP/p300 siRNAs significantly reduced SREBP promoter activities and mRNA levels (Fig. 5d, 6a and Supplementary Fig. 11c, d). We showed that IKK $\alpha$  exerts its effect on SREBP induction and lipogenesis through recruiting CBP/p300 complex. First, CBP/p300 depletion by siRNA significantly decreased cytosolic LD contents and HCV production (Fig. 6b, c). Second, siRNAs against CBP/p300 markedly diminished HCV 3'UTR-mediated SREBP-1 induction and LD formation (Supplementary Fig. 11d, e). Third, chromatin immunoprecipitation (ChIP) assay revealed that SREBP-1 promoter bindings of both IKK $\alpha$  and CBP were enhanced by HCV infection or HCV 3'UTR



transfection (Fig. 6d and Supplementary Fig. 11f). In addition, enhanced viral production by IKK $\alpha$  over-expression was substantially compromised in cells treated with CBP/p300 or SREBP siRNA (Fig. 6e), indicating that CBP/p300 and SREBPs are intimately involved in the IKK $\alpha$ -mediated proviral effect. Finally, to show that the DDX3X-IKK $\alpha$ -SREBP pathway is indeed crucial for productive HCV infection, we silenced these genes in combination and demonstrated that HCV infection was markedly reduced (>100-fold) as we knocked out the entire pathway (Supplementary Fig. 11g).

## DISCUSSION

Our study demonstrates a hitherto unrecognized function of IKK $\alpha$  in regulating cellular lipid metabolism and hence HCV assembly, both independent of its role in intrinsic innate immunity. We extensively validated and mechanistically investigated this novel function of IKK $\alpha$ . We showed that HCV, through the action of viral 3'UTR that contains a previously identified PAMP, specifically interacts with DDX3X and activates IKK $\alpha$  to mediate an NF- $\kappa$ B-independent function in the nucleus. Recent accumulating evidence indicates an emerging role of DDX3X in innate immunity, although the precise mechanism remains unclear<sup>28,29</sup>. Other members of the DEAD box family including the well-known RLRs and recently identified DDX1, DDX21 and DHX36 are important intracellular PRRs for RNA viruses<sup>27</sup>. Although DDX3X has been suggested to function as a PRR<sup>28</sup>, direct evidence is lacking. Here we show that DDX3X specifically recognizes HCV 3'UTR as a possible PRR. Binding of HCV 3'UTR to DDX3X leads to activation of IKK $\alpha$ . HCV core protein has been shown to bind to DDX3X<sup>33</sup>, but this interaction is dispensable for HCV-triggered activation of DDX3X-IKK $\alpha$  pathway.

This novel pathway involving DDX3X and IKK $\alpha$  appears to be unique to HCV because genome-wide siRNA screens of several viruses including HIV-1, Dengue, West Nile virus and influenza virus using the same screening platform did not identify this pathway as a crucial host factor for these viruses<sup>38-41</sup>. Towards this end, a proposed model is generated to illustrate the mechanism of action for DDX3X and IKK $\alpha$  in HCV infection (Fig. 6f). Unlike other factors in the NF- $\kappa$ B activation pathway that are exclusively antiviral genes, IKK $\alpha$ , although capable of modestly inducing ISG expression (Supplementary Fig. 12e), exerts predominantly a proviral effect that targets the assembly stage of HCV life cycle by activating SREBP-mediated lipogenesis and LD biogenesis. It is worth noting here that various HCV proteins have also been implicated to interact with the host lipid metabolism to facilitate HCV assembly<sup>22,23</sup>, but our data indicate that the primary trigger of LD biogenesis is mediated by the viral 3'UTR and viral proteins mainly play a downstream role in viral assembly<sup>22,23</sup>.

RNA viruses selectively exploit host specific elements to form specialized organelles where cellular lipids are crucial in enhancing viral production. Dengue virus (DENV) infection launches an autophagy-mediated processing of LDs and triglycerides that is required for efficient viral replication<sup>42</sup>. West Nile virus infection stimulates cholesterol biosynthesis and redistributes cholesterol to viral RNA replication membranes<sup>43</sup>. Recently, HCV infection was shown to depend on PI4P lipid-enriched membranes and PI4KIII kinases for RNA

replication<sup>44</sup>. HCV infection also induces LD formation for productive virion assembly<sup>24</sup>. Cellular lipogenesis is coordinated with LD formation and maturation<sup>45</sup>.

HCV infection is associated with hepatic steatosis and insulin resistance<sup>4</sup>, presumably because of HCV-induced dysregulation of lipid metabolism. Hepatic steatosis substantially contributes to the progression of fibrosis in chronic hepatitis C patients<sup>46</sup>. Interestingly, hepatic activation of IKK $\beta$  and NF- $\kappa$ B has been implicated in the etiology of insulin resistance and T2D<sup>47,48</sup>. Targeted deletion or pharmacological inhibition of IKK $\beta$  can restore insulin sensitivity in obese mice or humans<sup>49,50</sup>. Recent genome-wide association studies have shown that single nucleotide polymorphisms in the *CHUK* (IKK $\alpha$ ) gene locus are associated with nonalcoholic fatty liver diseases<sup>51</sup>. As we functionally link IKK $\alpha$  to lipogenesis in hepatocytes, it will be interesting to investigate the interaction among the various IKKs in HCV-associated steatosis and insulin resistance as well as in general cellular metabolism.

IKK $\alpha$ , as part of the NF- $\kappa$ B activation pathway, is involved in host recognition and defense against pathogen infection. Here we show that IKK $\alpha$  plays an important role in constitutive maintenance of lipogenic gene expression and LD formation in hepatocytes, and its activation by HCV further stimulates the lipogenic pathways to facilitate viral assembly. We reason that IKK $\alpha$  and its associated pathways have a dual effect on HCV infection – an antiviral effect via the NF- $\kappa$ B pathway and a proviral effect via the lipogenic pathway - with the latter being the dominant pathway in our experimental models. IKK $\alpha$  signaling may therefore represent a pivotal mechanism whereby chronic infection and inflammation leads to dysregulated metabolisms that are implicated in the development of various chronic metabolic disorders<sup>52</sup>. Our findings offer crucial insights into the inflammatory origin of metabolic disease and pathogenic consequences of chronic viral infection as well as potential novel approaches to treatment<sup>14,53</sup>.

A comprehensive understanding of the crosstalk between HCV and host innate response and lipid metabolism may help identify novel and broadly active antiviral targets<sup>54</sup>. The discovery of a critical proviral function of IKK $\alpha$  offers therapeutic opportunities for IKK $\alpha$  inhibitors in the treatment of HCV infection. The demonstrated efficacy of commercially available inhibitors of IKK activities in blocking HCV infection in this study provides a proof-of-concept approach for novel HCV therapeutic development. Our study also presents the first evidence that HCV usurps intrinsic innate immune pathway for its own advantage and survival. Such an exploitation of host antiviral defense may underlie the mechanism whereby HCV infection has a high propensity for persistent infection in the presence of an active immune response.

## ONLINE METHODS

### siRNA transfection

siRNAs were transfected into Huh7.5.1 cells at a 50 nM final concentration, using a reverse transfection protocol employing Oligofectamine (Invitrogen) as previously described<sup>19</sup>. For PHHs, cells were seeded on 12-well plates at 500,000 cells per well and transfected with siRNA at a final concentration of 50 nM using RNAiMAX (Invitrogen). Unless otherwise



indicated, further treatments or assays were typically performed 72 h after siRNA transfection, when gene silencing efficiency reaches maximal.

### **HCV core staining part-one (early stage) and part-two (late stage)**

For part one, Huh7.5.1 cells were treated with indicated SMARTpool siRNAs at a concentration of 50 nM for 72 h, then infected with HCV JFH-1 strain. After 48 h, cells were stained and imaged for HCV core production. This part detects host factors involved in the early stages of viral life cycle, from entry to viral protein translation and RNA replication. Culture supernatants of part one cells were transferred and infected naïve Huh7 cells, starting part two, which detects proteins involved in the later stages of viral infection, including virion assembly and release. siRNAs against CD81 and ApoE served as proviral controls for part one and part two respectively. Detailed protocol of core staining is described in the Supplementary Methods.

### ***In Vitro* transcription and labeling of HCV RNA and transfection**

Plasmids carrying JFH1, J6/JFH1 or Luc-JFH1/P7 genomic RNA or subgenomic replication RNA sequences were linearized with Xba I and purified by phenol-chloroform-isoamyl alcohol extraction. *In vitro* transcription was performed by using the MEGAscript T7 kit (Ambion), according to the manufacturer's protocol. The quality and quantity of RNA were evaluated by NanoDrop spectrophotometer (Thermo Scientific). Aliquots (22 $\mu$ l, 1  $\mu$ g  $\mu$ l<sup>-1</sup>) of RNA were stored frozen at -80 °C until use. HCV 3'UTR RNA was generated from a plasmid harboring the 3'-UTR of HCV that contains a poly-U/C region previously defined as the viral PAMP<sup>25</sup>. Cy3 labeling of RNA was conducted using Silencer siRNA labeling kit-Cy3 (Ambion). Biotin-labeled RNA was generated by including biotin-UTP (Roche; 1:6 ratio to UTP) during the synthesis process. RNA transfection was performed using DMRIE-C Reagent (Invitrogen) according to the manufacturer's instructions.

### **HCV life cycle assays**

HCV life cycle assays were performed using HCV pseudoparticles (for viral entry) and subgenomic replicons (for viral IRES-mediated translation and RNA replication), and single cycle infection assays were conducted using CD81-deficient Huh7-25 cells transfected with JFH1/P7-Luc or J6/JFH1 RNA. Detailed protocols for various assays are described in the Supplementary Methods.

### **Immunofluorescence, lipid staining, confocal microscopy and quantification of images**

Cells grown on Lab-Tek®II borosilicate 4-well chamber coverslips (Nunc) were fixed with 4% paraformaldehyde, permeabilized in 0.3% Triton X-100, and incubated with blocking solution in PBS containing 3% BSA and 10% normal goat serum (Vector Laboratories). Cells were then labeled with appropriate primary antibodies diluted in PBS with 1% BSA, followed by incubation with Alexa Fluor 488, 568 or 647 secondary antibodies (Invitrogen) in PBS with 1% BSA. Nuclei were counterstained with Hoechst 33342 (Invitrogen) at 1:5,000 in PBS. LDs were stained with BODIPY 493/503 (Invitrogen), applied at 1  $\mu$ g ml<sup>-1</sup> for 1 h in PBS with 1% BSA. Each step was followed by three washes with PBS. Confocal laser scanning microscopy analysis was performed with an Axio Observer.Z1 microscope

equipped with a Zeiss LSM 5 Live DuoScan System under an oil-immersion 1.4 NA 63× objective lens (Carl Zeiss). Images were acquired using ZEN 2009 software (Carl Zeiss). Dual or triple color images were acquired by consecutive scanning with only one laser line active per scan to avoid cross-excitation. Quantification of LDs was performed with ImageJ (National Institutes of Health), ZNF2009, and a set of defined intensity thresholds that were applied to all images.

### Microarray analysis

Huh7.5.1 cells were transfected with NT or IKK $\alpha$  siRNA for 72 h, then were mock-infected or infected with HCV at an MOI of 1. 48 h later, cellular RNA was extracted and purified using RNeasy Mini Kit (Qiagen). RNA was quantified with a spectrophotometer, and the RNA quality was analyzed with an Agilent Bioanalyzer according to the manufacturer's instructions. RNA was then amplified with an Agilent Enzo kit. Amplified complementary RNA was hybridized to an Affymetrix Human 133 Plus 2.0 microarray chip containing 54,675 gene transcripts. Microarray analyses were performed at the NIDDK Microarray Core Facility. The bioinformatics and statistical analysis were described previously<sup>55</sup>. A >1.5-fold change in expression combining a greater than 95% probability of being differentially expressed ( $P < 0.05$ ) was considered to be biologically significant. The infectivity of JFH-1 virus for Huh7.5.1 cells was tested prior to the microarray experiment.

### Gene expression assay

Total cellular RNA from a replica experiment was prepared with RNeasy Mini Kit (Qiagen). Complementary DNA (cDNA) was synthesized from total RNA with First Strand cDNA Synthesis Kit (Roche). The mRNA expression levels of target genes were quantified by quantitative PCR using gene-specific primers and probes (IDT) and TaqMan Gene Express Master Mix (Applied Biosystems) on an ABI 7500 Real Time PCR System. Relative transcript levels were calculated using the  $CT$  method, with 18S rRNA as the normalizing control gene.

### ChIP assays

ChIP assays were performed using SimpleChIP® Enzymatic Chromatin IP Kit (#9003, Cell Signaling) as described by manufacturers. In brief, after cross-linking, nuclei were purified and chromatin was sheared by sonication (three times, 20 s each). Chromatin was incubated overnight with specific antibodies against IKK $\alpha$  (ab4111, Abcam), CBP (ab2832, Abcam), and RNA-Polymerase II CTD (MA1-46093, Thermo Scientific). Isotype IgG were used as a negative control for the immunoprecipitation. Immunoprecipitated chromatin was then incubated with protein G magnetic beads, washed and eluted. After reversal of the cross-links and purification of DNA, precipitated DNAs were analysed by quantitative real-time PCR (40 cycles) with specific primers to the human actin promoter as a negative control, the IL-8 promoter as a positive control<sup>17</sup>, and SREBP-1 promoter (5'-GCTGTCCCGTGTTAGCCCTT-3' and 5'-TCTACCCGGGAGGTAGGGA-3'). Quantitative real-time PCR was performed in duplicate on duplicate ChIP on duplicate assays by using 500 nM of the above oligonucleotide primers and input DNA standards diluted in 5-fold increments from 5% to 0.008% with SYBR® Green PCR Master Mix

(#4309155, Applied Biosystems) and Applied Biosystems 7500 Sequence Detection System. Fold-increase of association of IKK $\alpha$ , CBP and Pol II to IL-8 and SREBP-1 promoters were normalized to actin signals and calculated for HCV-infected and HCV PAMP RNA-transfected cells as compared to untreated cells. *P* value was calculated using the Student's *t* test.

### Chemical inhibitor studies

IKK inhibitors II (Wedelolactone), XII, and III (BMS-345541) were purchased from Merck (EMD) Chemicals. Serial dilutions of the IKK inhibitors were made in 100% dimethyl sulfoxide (DMSO) immediately prior to the assay so that the final concentration of DMSO in each reaction was identical. Cells were infected with JFH-1 at an MOI of 0.5 for 6 h, and then treated with fresh DMEM containing DMSO with or without IKK inhibitors. Cultures were incubated for 48 h, and HCV RNA was extracted from cell lysate or culture medium and quantified by TaqMan real-time PCR. The experiments were done in triplicate, and each dose was tested at least twice.

### Additional methods

Detailed methodology is described in the Supplementary Methods.

### Supplementary Material

Refer to Web version on PubMed Central for supplementary material.

### ACKNOWLEDGMENTS

We thank Z. Hu, Y.-Y. Zhang, Y.-M. Li, E. Thomas, V. Gonzalez-Munoz and L. Holz for technical assistance, Y.-P. Wu of the NIDDK Confocal Microscopy Core for helping with confocal imaging, W.-P. Chen of the NIDDK Microarray Core Facility for DNA microarray analysis. We also thank A. Patel of University of Glasgow for providing the HCV core mutant (F24Y) virus. This work was supported by the Intramural Research Program of the National Institute of Diabetes and Digestive and Kidney Diseases, US National Institutes of Health. Primary human hepatocytes were provided by the NIH funded Liver Tissue Procurement and Cell Distribution System (N01-DK-7-0004/HHSN26700700004C, PI-S. Strom, University of Pittsburgh).

### REFERENCES

1. Liang TJ, Rehermann B, Seeff LB, Hoofnagle JH. Pathogenesis, natural history, treatment, and prevention of hepatitis C. *Ann Intern Med.* 2000; 132:296–305. [PubMed: 10681285]
2. Liang TJ, Ghany MG. *N Engl J Med.* 2013 in press.
3. Rehermann B. Hepatitis C virus versus innate and adaptive immune responses: a tale of coevolution and coexistence. *J Clin Invest.* 2009; 119:1745–1754. [PubMed: 19587449]
4. Syed GH, Amako Y, Siddiqui A. Hepatitis C virus hijacks host lipid metabolism. *Trends Endocrinol Metab.* 2010; 21:33–40. [PubMed: 19854061]
5. Herker E, Ott M. Unique ties between hepatitis C virus replication and intracellular lipids. *Trends Endocrinol Metab.* 2011; 22:241–248. [PubMed: 21497514]
6. Diamond DL, et al. Temporal proteome and lipidome profiles reveal hepatitis C virus-associated reprogramming of hepatocellular metabolism and bioenergetics. *PLoS Pathog.* 2010; 6:e1000719. [PubMed: 20062526]
7. Horton JD, Goldstein JL, Brown MS. SREBPs: activators of the complete program of cholesterol and fatty acid synthesis in the liver. *J Clin Invest.* 2002; 109:1125–1131. [PubMed: 11994399]

8. Waris G, Felmler DJ, Negro F, Siddiqui A. Hepatitis C virus induces proteolytic cleavage of sterol regulatory element binding proteins and stimulates their phosphorylation via oxidative stress. *J Virol.* 2007; 81:8122–8130. [PubMed: 17507484]
9. Lerat H, et al. Hepatitis C virus proteins induce lipogenesis and defective triglyceride secretion in transgenic mice. *J Biol Chem.* 2009; 284:33466–33474. [PubMed: 19808675]
10. Bowie AG, Unterholzner L. Viral evasion and subversion of pattern-recognition receptor signalling. *Nat Rev Immunol.* 2008; 8:911–922. [PubMed: 18989317]
11. Hayden MS, Ghosh S. Shared principles in NF-kappaB signaling. *Cell.* 2008; 132:344–362. [PubMed: 18267068]
12. Perkins ND. Integrating cell-signalling pathways with NF-kappaB and IKK function. *Nat Rev Mol Cell Biol.* 2007; 8:49–62. [PubMed: 17183360]
13. Senftleben U, et al. Activation by IKKalpha of a second, evolutionary conserved, NF-kappa B signaling pathway. *Science.* 2001; 293:1495–1499. [PubMed: 11520989]
14. Pasparakis M. Regulation of tissue homeostasis by NF-kappaB signalling: implications for inflammatory diseases. *Nat Rev Immunol.* 2009; 9:778–788. [PubMed: 19855404]
15. Anest V, et al. A nucleosomal function for IkappaB kinase-alpha in NF-kappaB-dependent gene expression. *Nature.* 2003; 423:659–663. [PubMed: 12789343]
16. Birbach A, et al. Signaling molecules of the NF-kappa B pathway shuttle constitutively between cytoplasm and nucleus. *J Biol Chem.* 2002; 277:10842–10851. [PubMed: 11801607]
17. Yamamoto Y, Verma UN, Prajapati S, Kwak YT, Gaynor RB. Histone H3 phosphorylation by IKK-alpha is critical for cytokine-induced gene expression. *Nature.* 2003; 423:655–659. [PubMed: 12789342]
18. Huang WC, Ju TK, Hung MC, Chen CC. Phosphorylation of CBP by IKKalpha promotes cell growth by switching the binding preference of CBP from p53 to NF-kappaB. *Mol Cell.* 2007; 26:75–87. [PubMed: 17434128]
19. Li Q, et al. A genome-wide genetic screen for host factors required for hepatitis C virus propagation. *Proc Natl Acad Sci U S A.* 2009; 106:16410–16415. [PubMed: 19717417]
20. Zandi E, Rothwarf DM, Delhase M, Hayakawa M, Karin M. The IkappaB kinase complex (IKK) contains two kinase subunits, IKKalpha and IKKbeta, necessary for IkappaB phosphorylation and NF-kappaB activation. *Cell.* 1997; 91:243–252. [PubMed: 9346241]
21. Akazawa D, et al. CD81 expression is important for the permissiveness of Huh7 cell clones for heterogeneous hepatitis C virus infection. *J Virol.* 2007; 81:5036–5045. [PubMed: 17329343]
22. Miyanari Y, et al. The lipid droplet is an important organelle for hepatitis C virus production. *Nat Cell Biol.* 2007; 9:1089–1097. [PubMed: 17721513]
23. Herker E, et al. Efficient hepatitis C virus particle formation requires diacylglycerol acyltransferase-1. *Nat Med.* 2010; 16:1295–1298. [PubMed: 20935628]
24. McLauchlan J. Lipid droplets and hepatitis C virus infection. *Biochim Biophys Acta.* 2009; 1791:552–559. [PubMed: 19167518]
25. Saito T, Owen DM, Jiang F, Marcotrigiano J, Gale M Jr. Innate immunity induced by composition-dependent RIG-I recognition of hepatitis C virus RNA. *Nature.* 2008; 454:523–527. [PubMed: 18548002]
26. Rothenfusser S, et al. The RNA helicase Lgp2 inhibits TLR-independent sensing of viral replication by retinoic acid-inducible gene-I. *J Immunol.* 2005; 175:5260–5268. [PubMed: 16210631]
27. Zhang Z, et al. DDX1, DDX21, and DHX36 helicases form a complex with the adaptor molecule TRIF to sense dsRNA in dendritic cells. *Immunity.* 2011; 34:866–878. [PubMed: 21703541]
28. Oshiumi H, Sakai K, Matsumoto M, Seya T. DEAD/H BOX 3 (DDX3) helicase binds the RIG-I adaptor IPS-1 to up-regulate IFN-beta-inducing potential. *Eur J Immunol.* 2010; 40:940–948. [PubMed: 20127681]
29. Schroder M, Baran M, Bowie AG. Viral targeting of DEAD box protein 3 reveals its role in TBK1/IKKepsilon-mediated IRF activation. *EMBO J.* 2008; 27:2147–2157. [PubMed: 18636090]
30. Ariumi Y, et al. DDX3 DEAD-box RNA helicase is required for hepatitis C virus RNA replication. *J Virol.* 2007; 81:13922–13926. [PubMed: 17855521]

31. Randall G, et al. Cellular cofactors affecting hepatitis C virus infection and replication. *Proc Natl Acad Sci U S A*. 2007; 104:12884–12889. [PubMed: 17616579]
32. Oshiumi H, et al. Hepatitis C virus core protein abrogates the DDX3 function that enhances IPS-1-mediated IFN-beta induction. *PLoS One*. 2010; 5:e14258. [PubMed: 21170385]
33. Angus AG, et al. Requirement of cellular DDX3 for hepatitis C virus replication is unrelated to its interaction with the viral core protein. *J Gen Virol*. 2010; 91:122–132. [PubMed: 19793905]
34. Reed BD, Charos AE, Szekely AM, Weissman SM, Snyder M. Genome-wide occupancy of SREBP1 and its partners NFY and SP1 reveals novel functional roles and combinatorial regulation of distinct classes of genes. *PLoS Genet*. 2008; 4:e1000133. [PubMed: 18654640]
35. Ericsson J, Edwards PA. CBP is required for sterol-regulated and sterol regulatory element-binding protein-regulated transcription. *J Biol Chem*. 1998; 273:17865–17870. [PubMed: 9651391]
36. Oliner JD, Andresen JM, Hansen SK, Zhou S, Tjian R. SREBP transcriptional activity is mediated through an interaction with the CREB-binding protein. *Genes Dev*. 1996; 10:2903–2911. [PubMed: 8918891]
37. Giandomenico V, Simonsson M, Gronroos E, Ericsson J. Coactivator-dependent acetylation stabilizes members of the SREBP family of transcription factors. *Mol Cell Biol*. 2003; 23:2587–2599. [PubMed: 12640139]
38. Brass AL, et al. Identification of host proteins required for HIV infection through a functional genomic screen. *Science*. 2008; 319:921–926. [PubMed: 18187620]
39. Sessions OM, et al. Discovery of insect and human dengue virus host factors. *Nature*. 2009; 458:1047–1050. [PubMed: 19396146]
40. Krishnan MN, et al. RNA interference screen for human genes associated with West Nile virus infection. *Nature*. 2008; 455:242–245. [PubMed: 18690214]
41. Brass AL, et al. The IFITM proteins mediate cellular resistance to influenza A H1N1 virus, West Nile virus, and dengue virus. *Cell*. 2009; 139:1243–1254. [PubMed: 20064371]
42. Heaton NS, Randall G. Dengue virus-induced autophagy regulates lipid metabolism. *Cell Host Microbe*. 2010; 8:422–432. [PubMed: 21075353]
43. Mackenzie JM, Khromykh AA, Parton RG. Cholesterol manipulation by West Nile virus perturbs the cellular immune response. *Cell Host Microbe*. 2007; 2:229–239. [PubMed: 18005741]
44. Hsu NY, et al. Viral reorganization of the secretory pathway generates distinct organelles for RNA replication. *Cell*. 2010; 141:799–811. [PubMed: 20510927]
45. Farese RV Jr, Walther TC. Lipid droplets finally get a little R-E-S-P-E-C-T. *Cell*. 2009; 139:855–860. [PubMed: 19945371]
46. Asselah T, Rubbia-Brandt L, Marcellin P, Negro F. Steatosis in chronic hepatitis C: why does it really matter? *Gut*. 2006; 55:123–130. [PubMed: 16344578]
47. Cai D, et al. Local and systemic insulin resistance resulting from hepatic activation of IKK-beta and NF-kappaB. *Nat Med*. 2005; 11:183–190. [PubMed: 15685173]
48. Yuan M, et al. Reversal of obesity- and diet-induced insulin resistance with salicylates or targeted disruption of Ikkbeta. *Science*. 2001; 293:1673–1677. [PubMed: 11533494]
49. Arkan MC, et al. IKK-beta links inflammation to obesity-induced insulin resistance. *Nat Med*. 2005; 11:191–198. [PubMed: 15685170]
50. Zhang X, et al. Hypothalamic IKKbeta/NF-kappaB and ER stress link overnutrition to energy imbalance and obesity. *Cell*. 2008; 135:61–73. [PubMed: 18854155]
51. Romeo S, et al. Genetic variation in PNPLA3 confers susceptibility to nonalcoholic fatty liver disease. *Nat Genet*. 2008; 40:1461–1465. [PubMed: 18820647]
52. Hotamisligil GS. Inflammation and metabolic disorders. *Nature*. 2006; 444:860–867. [PubMed: 17167474]
53. Baker RG, Hayden MS, Ghosh S. NF-kappaB, inflammation, and metabolic disease. *Cell Metab*. 2011; 13:11–22. [PubMed: 21195345]
54. Munger J, et al. Systems-level metabolic flux profiling identifies fatty acid synthesis as a target for antiviral therapy. *Nat Biotechnol*. 2008; 26:1179–1186. [PubMed: 18820684]

55. Feld JJ, et al. Hepatic gene expression during treatment with peginterferon and ribavirin: Identifying molecular pathways for treatment response. *Hepatology*. 2007; 46:1548–1563. [PubMed: 17929300]

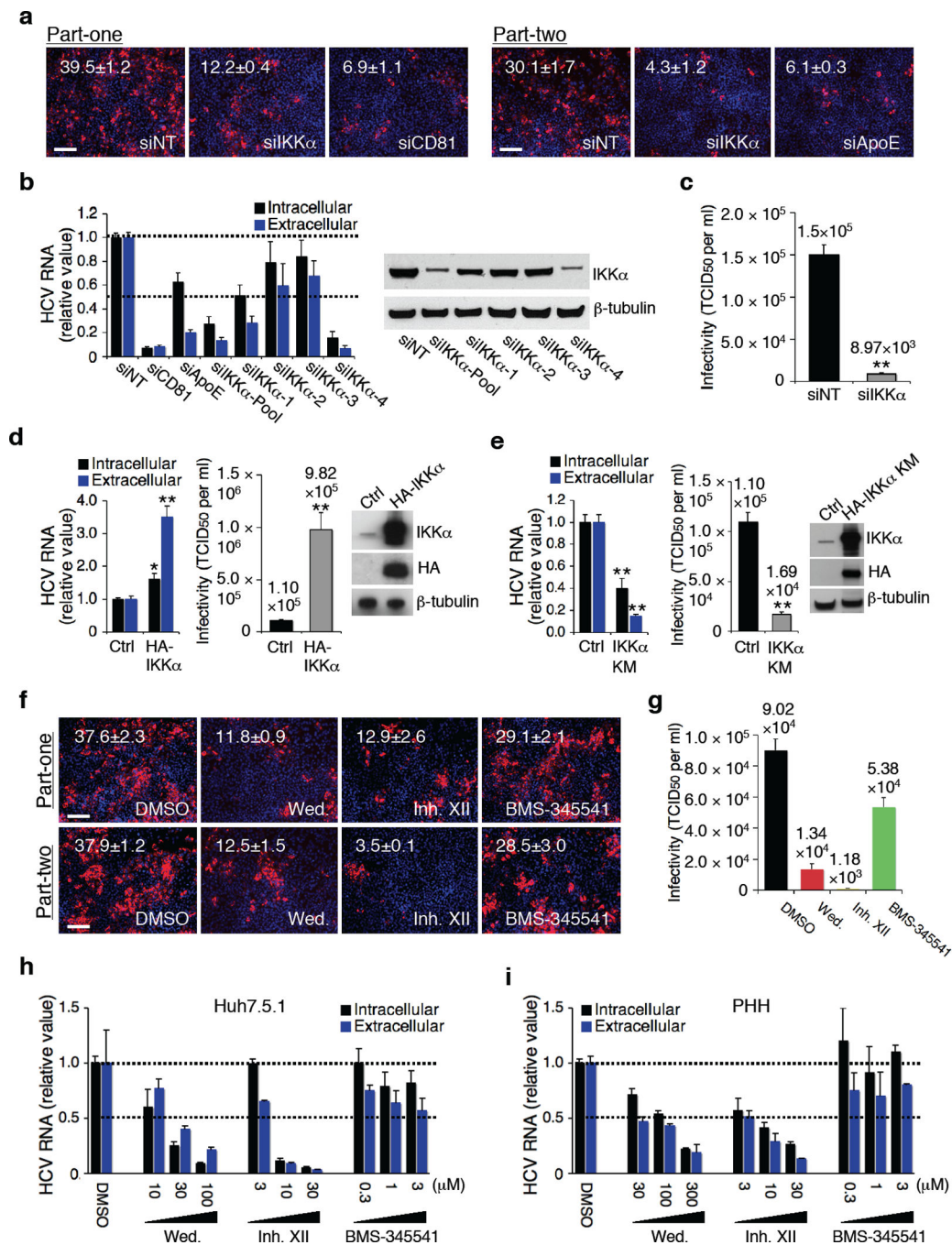
Author Manuscript

Author Manuscript

Author Manuscript

Author Manuscript



**Figure 1.**

Role IKK $\alpha$  in HCV infection. (a) Image illustration and quantitative analyses of HCV core staining part-one and part-two. Red: HCV core, blue: cell nuclei. Magnification 20 $\times$ . (b) Efficacies of various IKK $\alpha$  siRNAs in silencing IKK $\alpha$  and restraining HCV RNA production. Values were normalized as relative to nontargeting siRNA (siNT) control. (c) Effect of IKK $\alpha$  depletion on infectious HCV production and secretion, assessed by limiting dilution assay. (d) Effect of over-expression of IKK $\alpha$  on HCV infection. (e) Effect of over-expression of the kinase-defective HA-IKK $\alpha$  KM on HCV infection. (f,g) Effects of

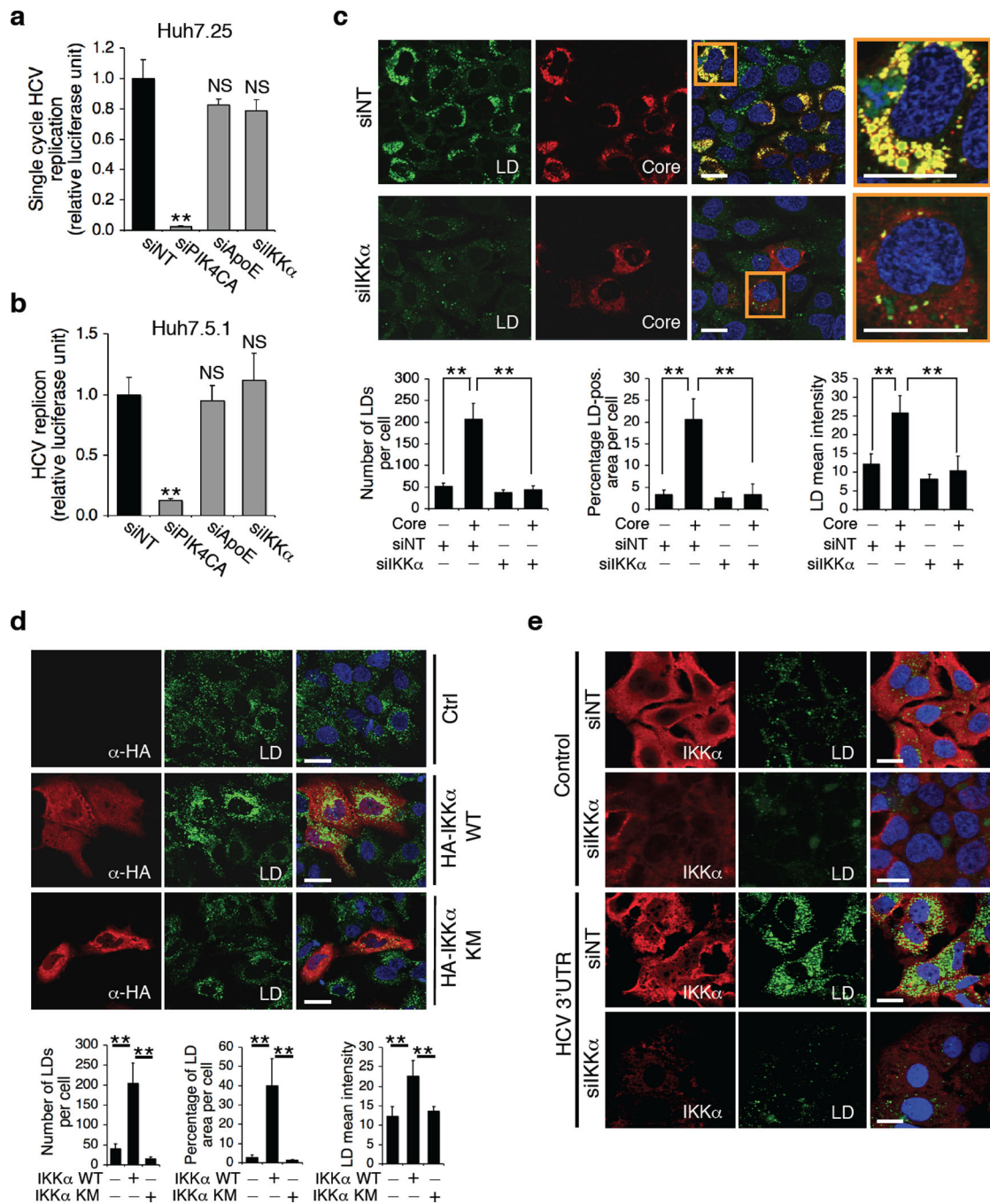
wedelolactone (30  $\mu\text{M}$ ) and IKK inhibitor XII (10  $\mu\text{M}$ ) on HCV production (**f**) and viral infectivity (**g**). (**h,i**) Dose-response effects of wedelolactone and IKK inhibitor XII on HCV RNA production and secretion in Huh7.5.1 cells (**h**) and PHHs (**i**). Error bars represent  $\pm$  s.d. of triplicate experiments. (**a,f**) Scale bars represent 100  $\mu\text{m}$ .

Author Manuscript

Author Manuscript

Author Manuscript

Author Manuscript

**Figure 2.**

IKK $\alpha$  function in HCV assembly and HCV-induced LD formation. **(a)** Effects of various siRNAs on HCV JFH-1/P7-Luc RNA replication in CD81-deficient Huh7.25 cells. **(b)** Effects of various siRNAs on HCV subgenomic replicon assay. **(a,b)** Values were normalized as relative units to siNT control, and error bars represent  $\pm$  s.d. of quintuplicate experiments. **(c)** LD contents (BODIPY) and HCV core expression in Huh7.5.1 cells treated with siNT or siIKK $\alpha$ . LD number: mean of >150 cells  $\pm$  s.d. Percent of LD-positive area: mean of >150 cells  $\pm$  s.d. LD mean fluorescence intensity: mean of >300 cells  $\pm$  s.d. **(d)**

Huh7.5.1 cells were transfected with control, HA-IKK $\alpha$  WT or HA-IKK $\alpha$  KM plasmid and then stained for HA-tagged IKK $\alpha$  expression and LD contents. LD numbers, positive area and mean fluorescence intensity were quantified: mean of >30 cells per condition  $\pm$  s.d. (e) Effect of IKK $\alpha$  silencing on HCV 3'UTR-mediated elevation of LD contents in Huh7.5.1 cells. For all microscopic images, scale bars represent 20  $\mu$ m. \*\*,  $P < 0.01$ . NS, not significant.

Author Manuscript

Author Manuscript

Author Manuscript

Author Manuscript



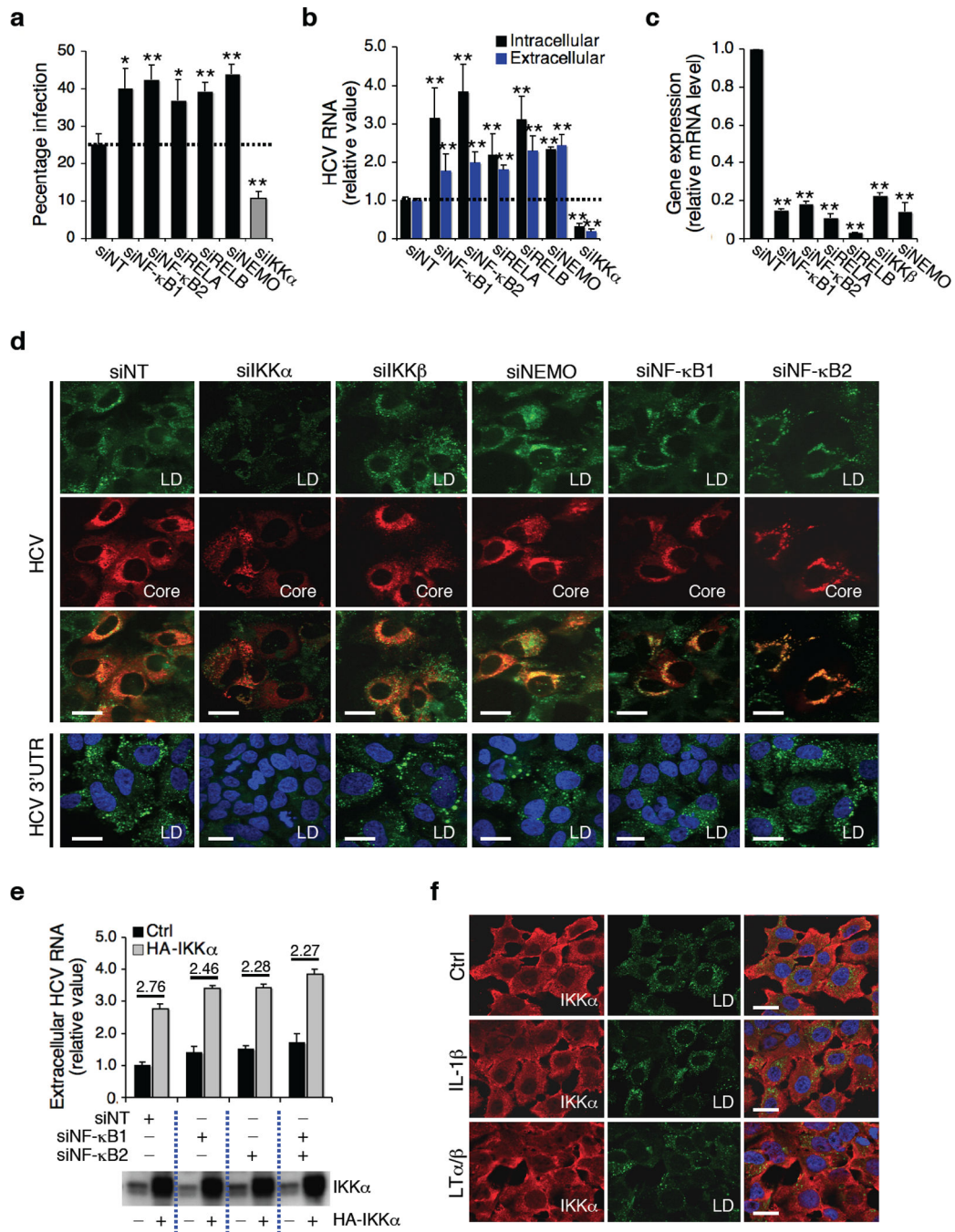


**Figure 3.** IKK $\alpha$ 's function and NF- $\kappa$ B pathway. **(a–c)** Effects of knockdown of NF- $\kappa$ B pathway on HCV infection. Values represent the means  $\pm$  s.d.,  $n = 3$ . \*\*,  $P < 0.01$ . **(d)** Effects of NF- $\kappa$ B silencing on HCV core-associated LD contents and 3'UTR-induced LD formation. **(e)** Huh7.5.1 cells were treated with indicated siRNAs, and then transfected with control or HA-IKK $\alpha$  plasmid before infection with HCV. Extracellular HCV RNA levels were subsequently measured and normalized to samples treated with siNT and control plasmid. **(f)**

Huh7.5.1 cells were incubated with IL-1 $\beta$  (0.1  $\mu\text{g ml}^{-1}$ ) or LT $\alpha/\beta$  (0.1  $\mu\text{g ml}^{-1}$ ) for 30 min, and stained for LD contents and IKK $\alpha$ . Scale bars represent 20  $\mu\text{m}$ .

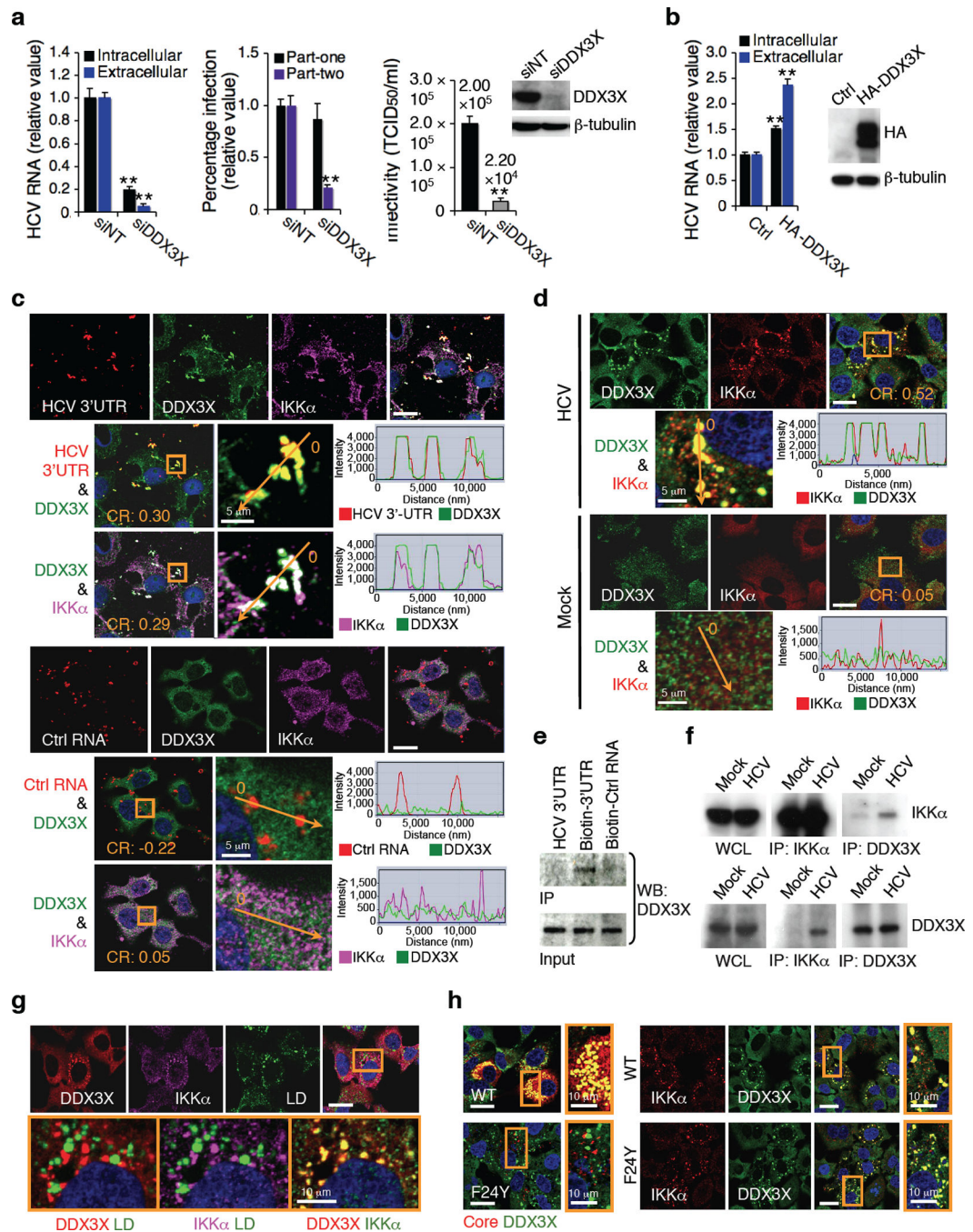
Author Manuscript

Author Manuscript

Author Manuscript

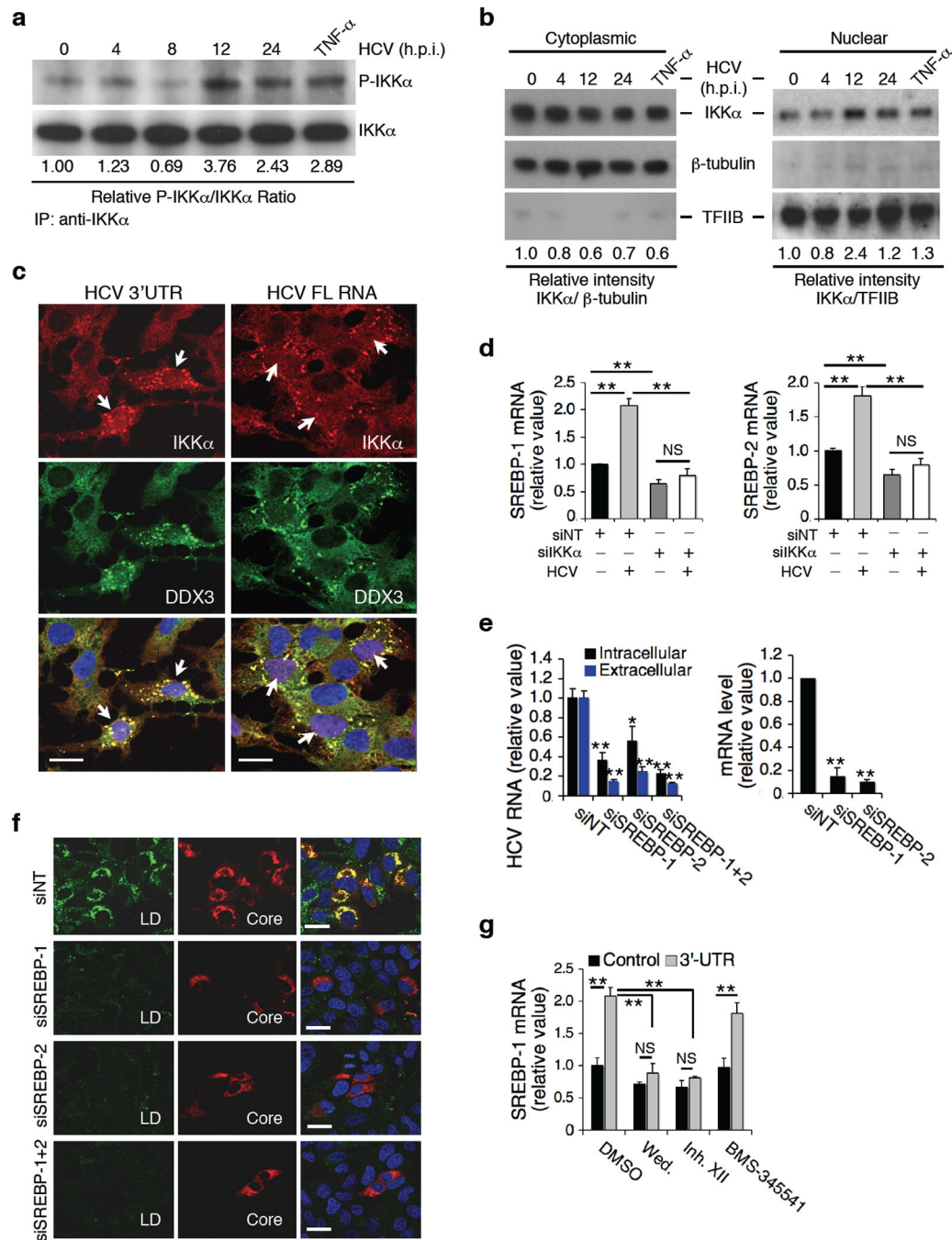
Author Manuscript



**Figure 4.**

Interaction of DDX3X with HCV 3'UTR and its role in HCV infection. **(a)** Effect of DDX3X siRNA on HCV RNA production, infectious HCV production as determined by part-two core staining and HCV infectivity (left, middle, and right panels, respectively). **(b)** Effect of over-expression of DDX3X on HCV RNA production. **(a,b)** Error bars represent  $\pm$  s.d. of triplicate experiments. \*\*,  $P < 0.01$ . **(c)** Cy3-labelled RNA was transfected into Huh7.5.1 cells for 4 h and examined by confocal microscopy for co-localization with DDX3X and IKK $\alpha$ . The control RNA is derived from a negative-strand transcript of an

EGFP plasmid. **(d)** HCV infection and DDX3X and IKK $\alpha$  co-localization in Huh7.5.1 cells. **(c,d)** The orange arrow or box corresponds to the co-localization analysis of fluorescence intensities that were measured by ZNF2009 software, and shown next to each of the image. CR – Pearson's correlation coefficient (R). **(e)** Biotinylated RNA was bound to streptavidin beads, and incubated with lysate from Huh7.5.1 cells. Protein eluted from the beads was subjected to Western blot with  $\alpha$ -DDX3X antibody. **(f)** Association of DDX3X and IKK $\alpha$  in HCV-infected cells, determined co-immunoprecipitation. **(g)** Huh7.5.1 cells were transfected with HCV 3'UTR for 24 h, and then stained for DDX3X, IKK $\alpha$  and LDs. **(h)** Huh7.5.1 cells were transfected with wild-type (WT) HCV RNA or F24Y HCV RNA for 48 h, and then stained for core, DDX3X and IKK $\alpha$ . Unless otherwise indicated, scale bars represent 20  $\mu$ m.

**Figure 5.**

HCV infection, IKK $\alpha$  activation, SREBP induction and LD formation. **(a)** Effect of HCV infection or TNF- $\alpha$  treatment on phosphorylation of IKK $\alpha$ , as shown by immunoprecipitation followed by Western blot. Phospho-IKK $\alpha$  and IKK $\alpha$  bands were quantified using ImageJ software and the ratios of P-IKK $\alpha$  over IKK $\alpha$  are provided beneath the blots. **(b)** Nucleus/cytoplasm (N/C) ratio of IKK $\alpha$  determined by dividing the relative intensity of nuclear IKK $\alpha$  normalized to TFIIB over that of cytoplasmic IKK $\alpha$  normalized to  $\beta$ -tubulin. The highest N/C ratio was achieved at 12 h post-infection (3.98). Control TNF-

$\alpha$  treatment led to an increased N/C ratio of 2.15. **(c)** Huh7.5.1 cells were treated with HCV 3'UTR or full-length (FL) HCV RNA for 4 h, immunostaining for DDX3X and IKK $\alpha$  was performed. White arrows indicate nuclear translocation of IKK $\alpha$  in viral RNA-treated cells showing co-localization of IKK $\alpha$  and DDX3X. **(d)** SREBP expression in IKK $\alpha$ -deficient cells. SREBP mRNA levels were measured at 72 h after siRNA treatment, 24 h after HCV infection or after both treatments, and were normalized as relative values to siNT-treated samples in the absence of HCV infection. **(e,f)** Effects of SREBP silencing in Huh7.5.1 cells on HCV infection **(e)** and LD formation **(f)**. **(g)** Effects of various IKK inhibitors (wedelolactone, 30  $\mu$ M; IKK Inhibitor XII, 10  $\mu$ M; BMS-345541, 1 $\mu$ M) on HCV 3'UTR-mediated induction of SREBP-1. **(d,e,g)** Error bars represent  $\pm$  s.d. of triplicate experiments. \*\*,  $P < 0.01$ . \*,  $P < 0.05$ . NS, not significant. **(c,f)** Scale bars represent 20  $\mu$ m.



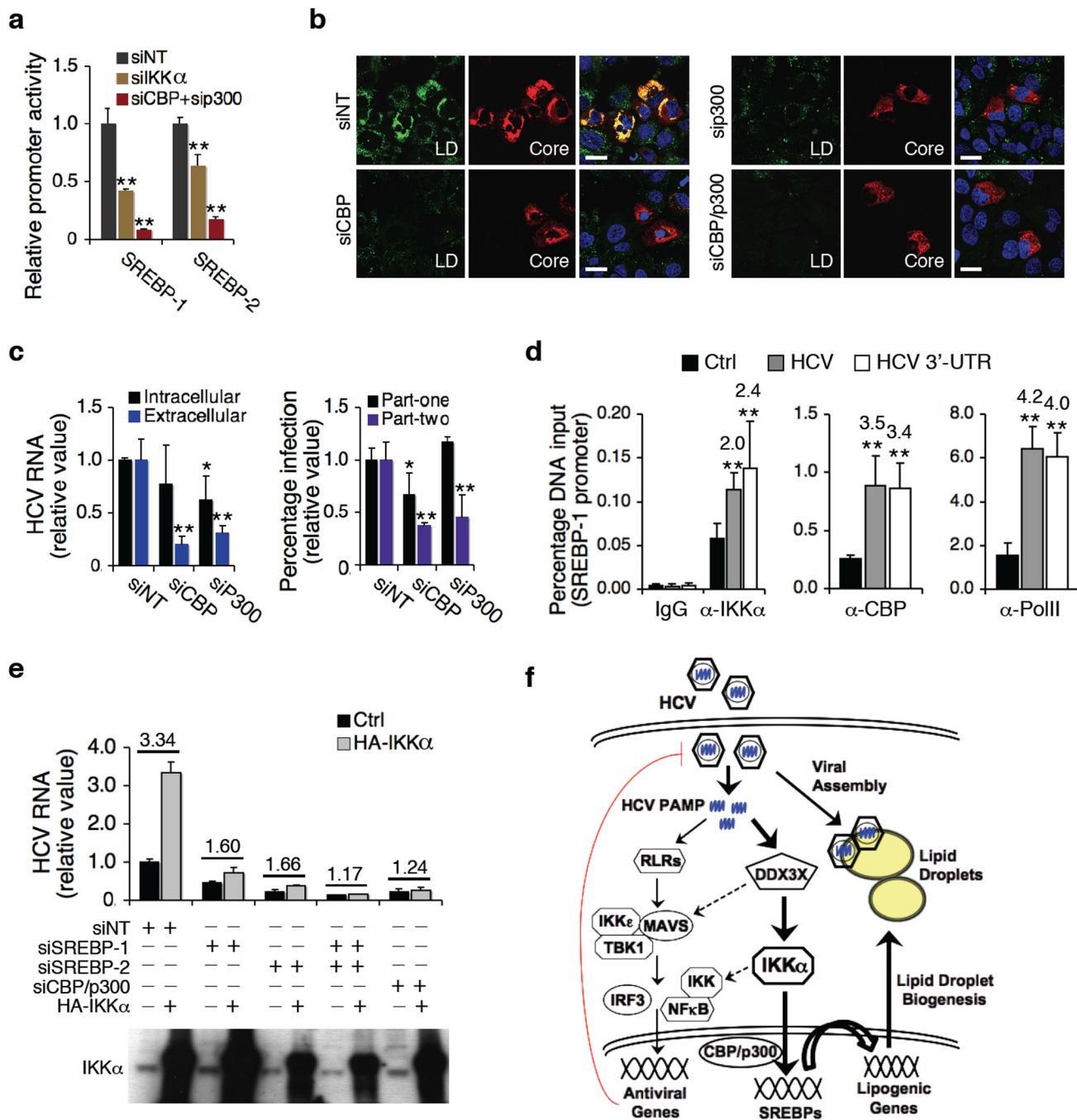


**Figure 6.** Signaling pathway involved in IKK $\alpha$ -mediated lipogenic induction of HCV infection. (a) Effects of IKK $\alpha$  or CBP/p300 siRNA on SREBP luciferase reporter activities. (b) LD contents and HCV core expression in CBP or p300 siRNA-treated Huh7.5.1 cells prior to HCV infection. Scale bars represent 20  $\mu$ m. (c) Effects of CBP/p300 silencing on HCV infection. Left: intracellular and extracellular HCV RNA levels; right: HCV core quantification in part-one and part-two of HCV cc assay. Western blot of CBP and p300 protein levels is shown in Supplementary Fig. 12c. (d) Huh7.5.1 cells were untreated,

infected with HCV or transfected with HCV 3'UTR RNA for 48 h, and chromatin immunoprecipitation (ChIP) assays were performed with the indicated antibodies. Only data for SREBP-1 promoter is shown here and data for IL-8 (positive control) and actin (negative control) promoters are shown in Supplementary Fig. 12d. Data are presented as means  $\pm$  s.d.,  $n = 4$ . (e) IKK $\alpha$  over-expression in HCV-infected cells deprived of SREBP-1, SREBP-2, or CBP/p300. (a,c,d,e) Error bars represent  $\pm$  s.d. of triplicate experiments. \*\*,  $P < 0.01$ , and \*,  $P < 0.05$ , as compared to control. (f) A proposed model of innate antiviral response and HCV-induced lipogenesis and LD formation in HCV assembly. The thickness of the arrows represents the putative magnitude of the two pathways (proviral > antiviral) in Huh7.5.1 cells. Dotted arrows represent possible cross-talks of the two parallel pathways.